Quaternary International 246 (2011) 124–133

Contents lists available at ScienceDirect

Quaternary International

journal homepage: www.elsevier.com/locate/quaint

Scale in tephrostratigraphic correlation: An example from Turkish Pleistocene archaeological sites

Christian A. Tryon [a,*], Steven L. Kuhn [b], Ludovic Slimak [c], M. Amelia V. Logan [d], Nur Balkan-Atlı [e]

[a] Center for the Study of Human Origins, Department of Anthropology, New York University, 25 Waverly Place, New York, NY 10003, USA
[b] Department of Anthropology, University of Arizona, Tucson, AZ 85721-0030, USA
[c] CNRS (UMR 5608), TRACES, Université de Toulouse le Mirail, France
[d] Department of Mineral Sciences, National Museum of Natural History, Smithsonian Institution, 10th and Constitution Ave. NW, MRC-119, Washington, DC 20560, USA
[e] Istanbul University, Faculty of Letters, Prehistory Section, Beyazit 34134, Istanbul, Turkey

ARTICLE INFO

Article history:
Available online 12 June 2011

ABSTRACT

Issues of scale are persistent but rarely made explicit in tephrostratigraphy. Eruption magnitude, the nature of available outcrop, and the resolution and type of data available define the scale of any proposed correlation. Different scales require different approaches to demonstrate, or more accurately, to estimate the likelihood of correlation among two or more deposits. This is emphasized through a probabilistic approach to the correlation of proximal and distal tephra deposits associated with Lower and Middle Paleolithic archaeological sites from central Turkey through the use of discriminant analyses and multiple analyses of variance.

1. Introduction

Tephra deposits are important stratigraphic markers because they may be widespread, are deposited rapidly, and often have a number of physical or chemical features that facilitate correlation of equivalent deposits even among widely separated outcrops. Just as the nature and magnitude of the tephra-producing geological events vary, the actual process of tephrostratigraphic correlation operates at a number of different spatial and analytical scales. For example, it is widely appreciated that fieldwork involves assessing variation at scales ranging from the source volcano, to outcrops of distal tephra, to the textural relations of individual volcaniclastic grains. Similarly, traditional methods of determining the geochemical composition of tephra include grain-discrete methods such as electron probe microanalysis (EPMA) best suited for measuring the relative weight percent abundances of major and minor elements, and bulk techniques that combine multiple grains into a single sample such as X-ray fluorescence (XRF) or instrumental neutron activation analysis (INAA) to measure trace elements measured in parts per million. More recent developments have moved towards the collection of trace element data from individual grains, particularly through the use of laser ablation inductively coupled mass spectrometry (Pearce et al., 2007; this issue).

Less widely appreciated is the fact that the methods of establishing the stratigraphic equivalence (correlation) among tephra deposits are scale dependent. The primary focus here is to demonstrate this through the use of numerical abundance data to establish correlations, first synthesizing available techniques, suggesting new directions forward, and using examples from Turkish Paleolithic archaeological sites as practical examples of the concepts discussed in this paper.

2. Scale in numerical correlation

Any stratigraphic correlation must be considered a testable hypothesis that is supported, rejected, or refined as relevant new data are collected. The most secure correlations employ multiple independent lines of evidence, including lithostratigraphic, chronological, and geochemical compositional data. Lithostratigraphic and chronological methods of demonstrating the equivalence of pyroclastic deposits use methods that are either widely used in sedimentary geology or are beyond the scope of the present paper; the focus instead is on the use of geochemical compositional data to correlate volcaniclastic deposits as this approach is particular to tephrostratigraphy.

Tephra consists of three components potentially useful to establish correlations between exposures in the field: the glass, crystal, and lithic phases (Schmid, 1981). The composition of the vitric (glass)

* Corresponding author. Fax: +1 212 995 4014.
E-mail addresses: christian.tryon@nyu.edu (C.A. Tryon), skuhn@email.arizona.edu (S.L. Kuhn), slimakl@yahoo.fr (L. Slimak), logana@si.edu (M.A.V. Logan), nbalkan@istanbul.edu.tr (N. Balkan-Atlı).

1040-6182/$ – see front matter © 2011 Elsevier Ltd and INQUA. All rights reserved.
doi:10.1016/j.quaint.2011.05.039

phase of tephra is commonly used to correlate widespread deposits. Volcanic glass reflects the composition of the magma at eruption, and the complexity of magmatic processes provides a potentially unique signature or 'fingerprint' for each volcano or eruption. Correlations exclusively based on crystal or lithic composition are less common, but these phases are equally useful as complementary data or where glass is not preserved (cf. McHenry et al., 2008; McHenry and Luque, 2011; Smith et al., this issue). However, most correlations between tepha deposits are based on glass geochemical composition because (1) glass composition is highly variable relative to that of the crystal and lithic phases, and (2) density separation results in the fallout of lithic and crystal phases closer to the source volcano, such that many distal deposits consist largely or solely of fine-grained glass shards.

A number of methods are currently in use to determine the degree of similarity among two or more tephra deposits from the geochemical composition of the vitric phase: these are reviewed or critiqued in greater detail by Lowe (2011), Denton and Pearce (2008), and Pearce et al. (2008). Here, three broad groups of related methods are recognized, summarized in Table 1. The first of these include exploratory methods designed to reveal the structure within a data set, including the use of various bivariate plots of element oxide wt. % abundances and cluster analysis (e.g., Campisano and Feibel, 2008). Bivariate plots are particularly effective at separating dissimilar deposits and cluster trees or dendrograms show an easy-to-grasp view of the relative ordering of similarity within a data set. Although they are visually intuitive, these methods do not provide robust means for assessing the degree of similarity among two or more samples. Consequently, bivariate plots and dendrograms are often applied in conjunction with other approaches.

The second group of methods provides a quantitative assessment of the degree of similarity among samples by computing a single value resulting from comparison of the mean values of the element oxide abundances within a sample. These statistics include the similarity coefficients of Borchardt et al. (1972) and the measure of Euclidean distance proposed by Perkins et al. (1995), both of which notably incorporate considerations of analytical precision into their comparison of sample means. Both methods remain in widespread use, but problems with the similarity coefficient approach can result when using sample means for heterogeneous eruptions (Riehle et al., 2008), and Denton and Pearce (2008) consider Euclidean distances as better at showing which deposits are not correlative rather than measuring similarity.

Table 1
Summary of different tephra correlation techniques and selected references. See text for discussion.

Technique	Selected References
Exploratory	
Bivariate plots	Tryon and McBrearty, 2006; Campisano and Feibel, 2008
Cluster analysis	Sarna-Wojcicki et al., 1984; Campisano and Feibel, 2008; Tryon et al., 2008
Single measure comparison	
Similarity coefficient	Borchardt et al., 1972; Sarna-Wojcicki et al., 1984; Kuehn and Foit, 2006; Riehle et al., 2008
Modified Euclidean distance	Perkins et al., 1995; Campisano and Feibel, 2008; Preece et al., in press
Variance comparison	
Elemental means overlap	Brown et al., 2006
t-test	Keenan, 2003
Bootstrap	Tryon et al., 2008
MANOVA	Tryon et al., 2010
Source attribution	
Discriminant analysis	Stokes and Lowe, 1988; Stokes et al., 1992

The third group of approaches incorporates within-sample grain-to-grain compositional variance into the comparisons, and focuses on estimation of the degree of uncertainty or statistical confidence in the proposed correlation. These include correlations based on one or more element oxide pairs whose means overlap at one standard deviation among two or more samples (Brown et al., 2006). More formal testing of the significance of this overlap may involve *t*-tests (Keenan, 2003), bootstrapping (Tryon et al., 2008), or multiple analyses of variance (MANOVA; Tryon et al., 2010). Discriminant analysis forms a subset of this third group of approaches. It has been used to develop a probabilistic framework to assign distal tephras to volcanic source, but it is applicable only where a large, comprehensive reference set of geochemically characterized proximal tephras of known origin exists (e.g., Stokes and Lowe, 1988; Stokes et al., 1992).

2.1. Which approach is 'correct'?

There is no single best method for correlating among tephra deposits on the basis of geochemical compositional data. The resolution of the data and the scale of the proposed questions determine which method is most appropriate, and indeed, different approaches can give different answers when applied to the same data set (e.g., Riehle et al., 2008; Tryon et al., 2008). A few examples serve to illustrate this point, working from the coarsely resolved scale of attributing tephra to volcanic source to correlating geographically widespread deposits from a single eruption.

Archaeologists working to identify the geological source of prehistoric stone tools or the clay used to manufacture pottery have long relied on the "provenance postulate" first formulated by Weigand et al. (1977), which simply recognizes that in order for a source attribution to be made among a number of possible options, inter-source variation must exceed intra-source variation. A similar logic has guided a number of tephrostratigraphic projects, founded on the observation that as different volcanic eruptions are compositionally distinct, so too are the signatures of particular volcanoes that undergo multiple eruptions over time. As noted above, discriminant analysis (or discriminant function analysis) is ideal for such settings. The method was originally developed for taxonomic applications in biology (Fisher, 1936), using metrical data to support species designations. It requires an *a priori* defined reference set, which in tephrostratigraphic applications is typically a group of geochemically characterized proximal tephra deposits that provide a measure of the compositional variation within a single volcanic source. Discriminant analysis (DA) provides a linear function or equation that best separates cases into the different pre-defined members of the reference set. Cross-validation methods (e.g., jackknifed subsamples) provide posterior probabilities based on the frequency with which samples within the reference set (the 'knowns') are correctly classified using this linear function or equation, providing a measure of the accuracy of the model in discriminating among different volcanic sources. Once the classificatory model or function has been defined based on the reference set, samples of unknown composition can be assigned to one of the volcanic sources, with estimates of the goodness of fit provided by posterior probabilities of classification, Mahalanobis distances from group centroids, and plots of canonical scores that reflect the linear combination of variables that best discriminate among the different groups. The primary drawback of the method is that distal tephra will only be assigned to sources within the pre-defined reference set, so that deposits from sources not included in the reference set will be misclassified. In situations where a well-defined reference set is lacking, principle components analysis or similar approaches may be warranted. Accessible but more detailed treatment of these issues may be found in Baxter (1994) and Feldesman (1997).

Stokes and Lowe (1988) provide the classic application of discriminant analysis in tephrostratigraphy. A robust program of EPMA of multiple deposits from each of the five major tephra-producing volcanoes on New Zealand's North Island provided a reference set to which distal tephras of unknown source could be compared. Discriminant analyses of the reference set indicated a correct classification rate from 91 to 100% and thus provide a high degree of confidence in the classification of the unknowns to volcanic source (Stokes and Lowe, 1988). Although the method readily distinguished among the different sources on the basis of between-volcano compositional variation, when applied to identify individual eruptions *within* each volcano, lower rates of correct classification (70–100%) resulted due to relatively reduced variation within the major and minor elements compared (Stokes et al., 1992). That is, following the logic of the provenance postulate, levels of intra-source variation approached those of inter-source variation at the volcano, reducing the discriminatory power of the method.

Although discriminant analysis is a powerful analytical tool useful in situations with a robust reference set, it is of little use in constructing stratigraphic frameworks in regions with distal tephra of unknown source. In these cases, different approaches must be adopted. At a relatively coarse scale, Tryon and McBrearty (2002, 2006) used a series of bivariate plots (Harker diagrams) to identify linear compositional trends among basaltic tephra from the middle Pleistocene Kapthurin Formation in Kenya. These showed that progressive changes in various element oxides occurred with increased stratigraphic height, likely the outcome of periodic eruptions from a source undergoing more or less continuous magmatic compositional change. Although up to seven basaltic tephra deposits occurred within a single stratigraphic section, these were assigned to a relative stratigraphic sequence composed of only three groups of increasingly evolved basaltic tephra. These groups were defined by gaps in the compositional range of multiple element oxides. More precise attempts to correlate among deposits, that is, to link deposits associated with particular eruptions rather than attributing them to broad compositional groups were unwarranted because (1) the number of analyses of each tephra deposit was low ($n \approx 5$), precluding the use of most statistical methods and (2) most of the tuffaceous beds recognized in the field were the result of secondary redeposition in a fluvial environment rather than primary tephra fallout, resulting in the occasional mixing of formerly discrete eruptive events.

Finally, correlating the deposits of individual eruptions has been a major focus of many tephrostratigraphic research projects, and the correct identification of a particular well-dated deposit can have important implications for regional chronologies of environmental or archaeological change: examples include the identification of deposits on the Indian subcontinent from eruptions of Toba (cf. Westgate et al., 1998; Williams et al., 2009; Chauhan, 2010) or those from the Campanian Ignimbrite, found across southern Eurasia (e.g., Fedele et al., 2008; Bourne et al., 2010). Because these are finer-scale questions, they require robust methods for establishing tephrostratigraphic equivalence. This is particularly the case when seeking to identify a particular eruption from a source with multiple candidate tephras distinguished only by subtle geochemical differences, as is true for the Campanian Province of Italy (Turney et al., 2008).

Tryon et al. (2010) provide one of the more extreme examples, using MANOVA to link Pleistocene distal tephra deposits from Rusinga Island, Kenya, in Lake Victoria. Proposed correlations are those for which the weight percent abundance of the sample means of *all* analyzed element oxides overlap at one standard deviation. These proposed correlations were then more formally tested using one-way MANOVA, a statistically conservative method related to discriminant analysis (Neff and Marcus, 1980) that compares the variance among element oxide means for each sample. The approach tests the hypothesis that sample means are different (representing more than one statistical population) and that different tephra beds are not correlative. Among samples for which three or more samples are being compared, *post hoc* Hotelling's T^2 tests can be used to determine if individual sample pairs are correlative even if significant differences are demonstrated for the larger data set. As for the one-way MANOVA, those samples or sample pairs that cannot be shown to be statistically different, that is for which the hypothesis of dissimilarity is rejected at $p > 0.05$, are considered correlates.

2.2. Numbers are not enough

Probabilistic approaches such as DA and MANOVA that suggest equivalence on the basis of multivariate analyses of complete data sets offer the strongest cases for tephra correlation. However, it is absolutely important to stress that whatever the degree of precision or confidence provided by any statistical method in tephra analyses, the generated results are meaningless in the absence of geological context. The accuracy of the proposed correlations must be assessed in concert with other lines of stratigraphic or chronological data, as well as consideration of evidence for other processes that may account for compositional variation among tephra deposits of the same eruption. These include but are not limited to (1) differential sampling of the eruptive products of heterogeneous magma batches (Riehle et al., 2008; Shane et al., 2008), (2) differential loss or uptake of particular elements (e.g., sodium) in varied depositional environments in which tephra may be found (Cerling et al., 1985), (3) data standardization procedures such as normalization to 100%, which may have proportionately different effects on analyses with low totals (cf. Brown et al., 1992; Hunt and Hill, 1993; Perkins et al., 1995; Pollard et al., 2006; Pearce et al., 2008), and (4) variation as a result of inter- or intra-laboratory variation (e.g., Jarosewich et al., 1979; Hunt and Hill, 1996; Jensen et al., 2008; Tryon et al., 2009; Bourne et al., 2010; Kuehn et al., this issue).

3. Pleistocene tephrostratigraphy at Turkish Paleolithic sites: variable scales, variable approaches

As an example of the effects of scale on the choice of analytical approach and the benefits of some statistical approaches to tephrostratigraphy, this paper describes ongoing research in the Central Anatolian Volcanic Province (CAVP) of Turkey (Fig. 1). The region itself is tectonically active and widely dispersed Pleistocene distal tephra are common, and our previous efforts have focused on building a basic tephrostratigraphic sequence for Paleolithic archaeological sites in the region. Excavated Paleolithic archaeological sites in Turkey are rare and chronological control is limited, although crucial to understanding the evolution and population histories of diverse hominin lineages, including *Homo erectus*, Neanderthals, and *Homo sapiens* (Otte et al., 1998; Kuhn, 2002, 2009; Kappelman et al., 2007; Slimak et al., 2008; Kuhn et al., 2009).

Previous work (Tryon et al., 2009) has focused on the ~4–5 m deep stratigraphic sequence of fallout and reworked tephra exposed at the Lower and Middle Paleolithic archaeological site of Kaletepe Deresi 3 (KD3, see Fig. 1). Discriminant analysis was used to attribute rhyolitic tephra deposits to different volcanic sources. Through extensive fieldwork and EPMA, Mouralis constructed a large database describing the compositional variation of the various Pleistocene tephra-producing volcanic centers in the region (Mouralis 2003; Mouralis et al., 2002; Slimak et al., 2008). Discriminant analysis demonstrated that these different sources, and in some cases, different eruptive phases within a source, could be reliably distinguished on the basis of major and minor element geochemical composition (~95–97% of the total sample correctly

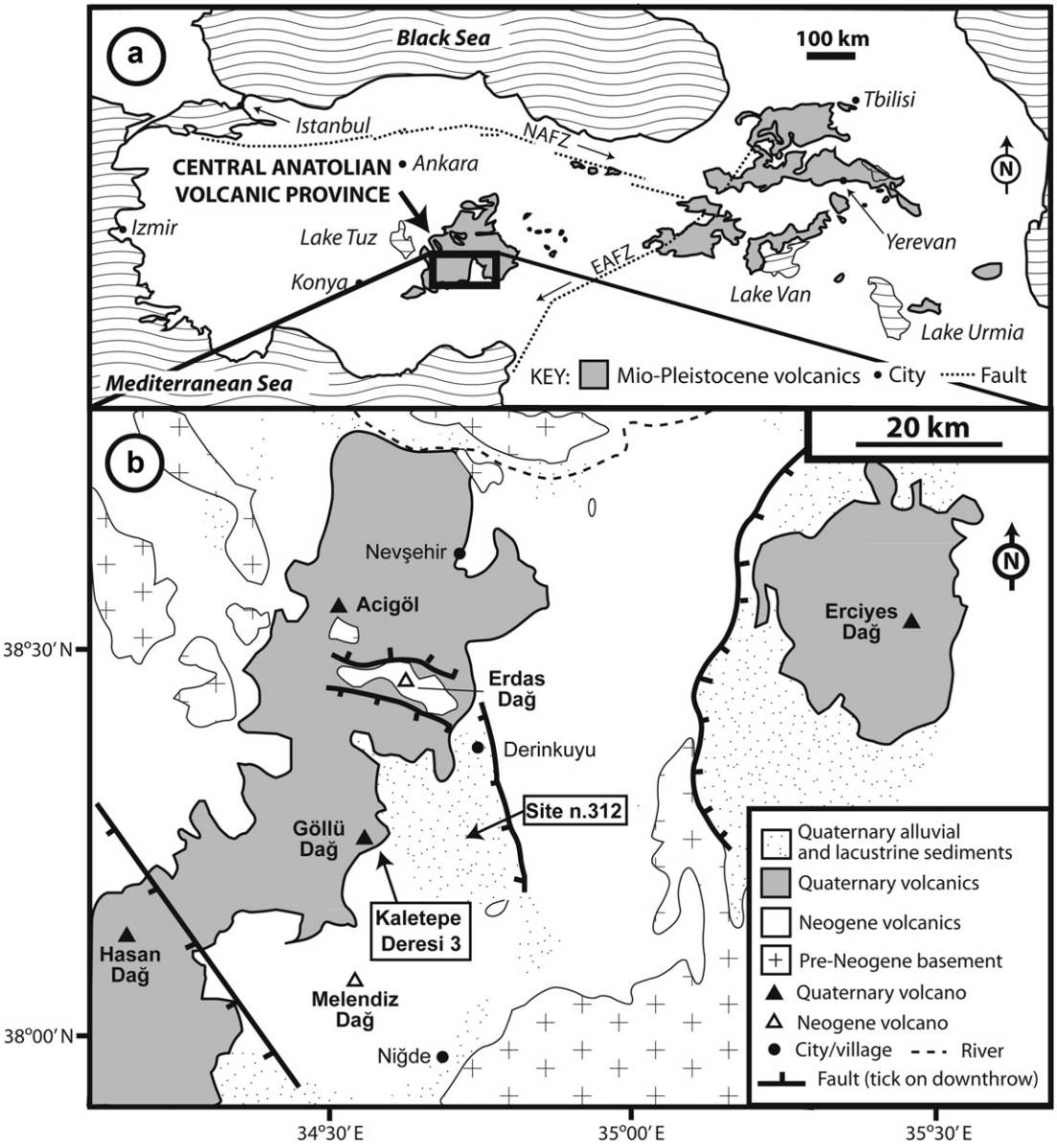

Fig. 1. (a) Schematic map showing the distribution of Quaternary volcanic rocks in Turkey and adjacent areas and the location of the Central Anatolian Volcanic Province (CAVP), modified after Innocenti et al. (1982) and Deniel et al. (1998). (b) Main geological features of the CAVP, including all Quaternary volcanic edifices that are potential sources of distal tephra, as well as the positions of archaeological sites Kaletepe Deresi 3 and n.312, after Druitt et al. (1995). Figure adapted from Tryon et al. (2009).

classified using jackknifed cross-validation). Individual grains ($n = 481$) were analyzed from the reworked deposits, and those that could confidently be attributed to source recorded a general succession of eruptive deposits from different volcanoes or eruptive events. Once the distal tephra were linked to source, age estimates of the volcanoes determined by prior researchers could be used to provide a coarse degree of chronological control for the middle and late Pleistocene sediments at KD3 (Tryon et al., 2009).

More recent survey in the CAVP has revealed that KD3 is only one of a number of Paleolithic archaeological sites in the region (Balkan-Atlı et al., 2008, 2009), and some of these archaeological localities are associated with tephra deposits. At one of these localities (n.312, see Fig. 1), Middle Paleolithic artifacts of obsidian, including Levallois flakes, scrapers, and cores are eroding from within an approximately 1.0-m-thick deposit of fine-grained mafic ash-fall deposit ~11.5 km east of KD3.

The mafic ash deposit at site n.312 (sample GS08-01) is locally distinctive, as the majority of the distal tephra in the area differ in color and grain size, being felsic (rhyolitic) lapilli-fall deposits. However, two deposits of macroscopically similar mafic tephra are found in the vicinity of KD3. The first of these is unit R6, a 15 cm thick bioturbated mafic ash-fall deposit that caps the stratigraphic sequence at KD3 sampled as CAT06-41T, where it is also associated with Middle Paleolithic artifacts in the adjacent *amont* and *aval* excavations at the site (see Slimak et al., 2008 for excavation details). Prior geochemical analyses of this deposit by EPMA identified its trachyandesitic composition (Mouralis et al., 2002; Tryon et al., 2009). Additional deposits of mafic ash were found in the upper part of the 2008 excavations at test excavation or *sondage* #2 in the KD3 area, sampled as CAT08-07. *Sondage* #2 is located approximately 28 m southeast and slightly downslope from the top of the *aval* excavation trench.

Electron probe microanalysis of the three mafic tephra samples tested the hypothesis that all are stratigraphically equivalent and derive from the same eruption. If this hypothesis is supported, these analyses expand the geographic scope of the tephrostratigraphic correlations. That is, rather than a focus on the sequence of tephra at a single site, the emphasis is shifted to the distribution of a single tephra deposit across multiple sites. This perspective broadens the scale of the archaeological comparisons beyond that of a single site to the wider study of ancient landscapes and associated spatial variation in human behavior, as has been successfully done, for example, in the Turkana Basin of Kenya and Ethiopia (e.g., Stern, 1993; Brown et al., 2006; Tiercelin et al., 2010).

Previous efforts had focused on the rhyolitic tephra deposits because of their greater abundance, and the presence of a well-defined reference set of source localities of rhyolitic tephra. The scale of the initial questions as well as the available comparative data facilitated use of disriminate analysis. Multiple samples of mafic ashes are now available for the first time, but the nature of the data set dictates a different approach designed to correlate among individual deposits.

3.1. Comparative sample

Comparison involved sample GS08-01 from site n.312, sample CAT06-41T from the *amont* and *aval* excavations at KD3, and sample CAT08-07 from sondage #2 at KD3. Each of these three lithologically distinct black, fine-grained tephra samples is similar in hand specimen and thin section. Careful visual inspection using backscattered electron imaging revealed two distinct shard populations in each sample. Shards of the first and numerically abundant population, shown in Fig. 2, have a vitrophyric texture with a high density of feldspar and Fe–Ti oxide microlites within a mafic glass groundmass. Shards of the second population are considerably more rare, are felsic, and lack phenocrysts. The felsic glass phase was noted during previous examination of CAT06-41T but was not reported in Tryon et al. (2009) because it was assumed that these grains were contaminants. Although careful sampling protocols were used from the start, the outcrop from which CAT06-41T derived included very unconsolidated tephra with abundant felsic deposits above and beneath it, increasing the likelihood of the accidental inclusion of detrital grains from neighboring strata during sample collection. However, the presence of the same bimodal distribution of glass types in all three mafic samples from widespread outcrops argues against accidental inclusion and suggests that the bimodal composition is a distinctive characteristic of these deposits.

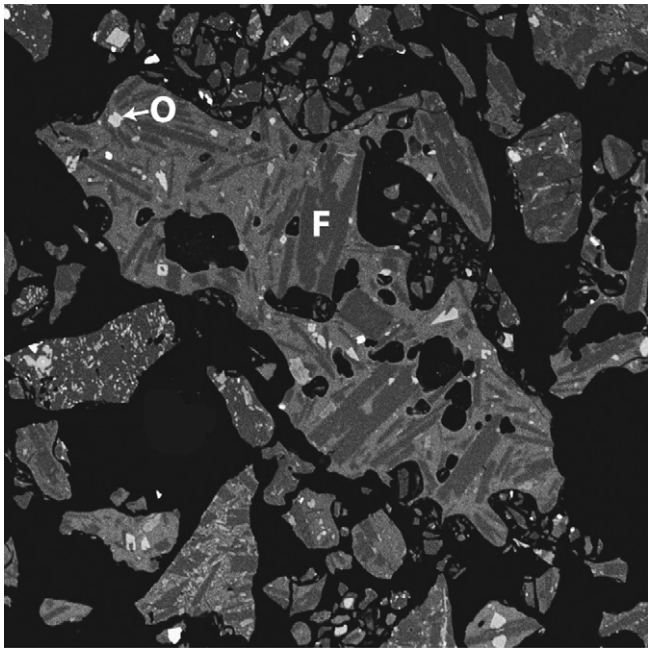

Fig. 2. Vitrophyric texture of sample CAT08-07 (sondage #2, Kaletepe Deresi 3) visible in backscattered electron image, with dense concentrations of feldspar laths (F) and Fe–Ti oxides (O) in a mafic glass groundmass. Width of field is 380 μm.

3.2. Analytical methods

Although the test focused on the hypothesized correlation of different deposits that may represent a single tephra fallout event, the bimodal distribution of mafic and felsic glass shards emphasizes the importance of a grain-discrete scale of analysis. Therefore, compositional data for between 5 and 14 shards of the mafic and felsic populations of each sample were acquired using wavelength dispersive quantitative analyses of major and minor element oxide abundances. Analyses were conducted using a JEOL 8900R electron microprobe, housed in the Mineral Sciences Department of the Smithsonian Institution's National Museum of Natural History, with a 40° take-off angle. Analytical conditions consisted of an accelerating voltage of 13 kV and a beam current of 10 nA, using a rasterized beam over an area of ~25 μm^2. Counting times were 20 s on-peak and 10 s off-peak. Reference materials used for calibration of the glass analyses include anorthite (USNM 137041), Kakanui hornblende (USNM 143065), microcline (USNM 143966), scapolite (USNM R6600-1), fayalite (USNM 85276), synthetic wollastonite and enstatite, as well as Yellowstone rhyolitic glass VG-568 (USNM 7285), characterized by Jarosewich et al. (1980). Raw data were converted to concentrations using standard calculations with the PhiRhoZ matrix correction of Armstrong/Love Scott (Armstrong, 1988). Optimal analytical conditions that minimize sample damage and volatile element loss or mobilization, particularly sodium, were achieved through an extensive testing program of analyzing USNM 7285 as an unknown (for discussion, see Hunt and Hill, 1996, 2001). A time dependent intensity correction with a 2 s interval was applied for Na, Si, and K using Probe for EPMA software (Donovan et al., 2009).

Results are summarized in Table 2 (raw data are available as Appendix 1). Samples with analytical totals <93% were culled from the data set. This value is arbitrary, but is above that recommended by Froggatt (1992), reflects a natural break in the distribution of analytical totals in the sample (see discussion in Pollard et al., 2006), and was chosen to increase the sample size of felsic grains, which on average had lower totals than the mafic ones. To remove potential issues of intra-laboratory variation (Jarosewich et al., 1979: 63–66; Perkins et al., 1995: 1504; Jensen et al., 2008: 413), sample CAT06-41T, originally analyzed in 2008, was reanalyzed in 2010 concurrent with samples CAT08-07 and GS08-01. Although only data collected in 2010 are used here, comparisons of normalized totals of the 2008 and 2010 analyses suggest good reproducibility (Table 2). The well-characterized The Yellowstone rhyolitic glass VG-568 (USNM 7285) and Kakanui hornblende (USNM 143065) reference materials were also analyzed as unknowns to facilitate inter-laboratory comparison, with results presented in Appendix 1. All statistical comparisons were made using PAST version 2.04 (Hammer et al., 2001) and Systat® version 12 software.

3.3. Results

As shown in Fig. 3, all distal tephra samples consist of trachyandesite and rhyolite glass populations according to normalized sample means plotted on the total-alkali silica diagram of Le Bas

Table 2
Summary electron probe microanalysis data, listed as mean and one standard deviation for each element oxide. Total listed is the sum of the average wt. % of each oxide, n = number of glass shards analyzed, FeO_T = total Fe expressed as FeO.

Sample	n	SiO_2	TiO_2	Al_2O_3	FeO_T	MnO	MgO	CaO	Na_2O	K_2O	Total
Mafic glass phase											
GS08-01	14	58.29±1.42	1.89±0.10	14.58±0.63	8.18±0.64	0.16±0.05	1.89±0.12	4.30±0.16	4.21±0.31	2.98±0.24	96.48
CAT08-07	14	59.41±1.06	1.78±0.13	14.93±0.72	7.58±0.60	0.16±0.06	1.84±0.29	4.08±0.54	4.42±0.27	3.01±0.31	97.21
CAT06-41T	9	59.46±1.27	1.91±0.08	14.05±0.22	7.91±0.46	0.12±0.07	1.89±0.11	4.27±0.20	4.50±0.42	2.81±0.30	96.93
Felsic glass phase											
GS08-01	8	71.55±0.85	0.07±0.02	13.14±0.45	1.07±0.30	0.08±0.05	0.05±0.02	0.67±0.20	3.86±0.23	4.51±0.16	94.99
CAT08-07	5	71.01±0.50	0.08±0.02	12.99±0.07	1.04±0.21	0.08±0.08	0.05±0.01	0.72±0.02	3.75±0.19	4.47±0.27	94.19
CAT06-41T	5	72.67±0.57	0.06±0.01	12.59±0.32	0.90±0.37	0.06±0.03	0.04±0.02	0.64±0.17	3.90±0.18	4.46±0.15	95.32
Normalized values											
Mafic glass phase											
GS08-01	14	60.42±0.52	1.96±0.13	15.11±0.51	8.47±0.61	0.16±0.06	4.46±0.20	1.96±0.13	4.37±0.33	3.09±0.25	100.00
CAT08-07	14	61.11±0.59	1.89±0.30	15.35±0.64	7.80±0.66	0.16±0.06	4.20±0.53	1.83±0.13	4.55±0.27	3.10±0.34	100.00
CAT06-41T	9	61.34±0.31	1.96±0.13	14.50±0.13	8.15±0.40	0.13±0.07	4.41±0.17	1.97±0.06	4.64±0.42	2.90±0.30	99.99
Felsic glass phase											
GS08-01	8	75.32±0.88	0.07±0.02	13.83±0.35	1.12±0.30	0.08±0.05	0.05±0.02	0.71±0.21	4.06±0.20	4.75±0.15	100.00
CAT08-07	5	75.39±0.36	0.08±0.02	13.79±0.09	1.11±0.22	0.09±0.09	0.06±0.01	0.77±0.03	3.98±0.21	4.75±0.28	100.00
CAT06-41T	5	76.25±0.65	0.07±0.02	13.21±0.31	0.94±0.39	0.06±0.03	0.04±0.02	0.67±0.18	4.09±0.18	4.68±0.16	100.00

et al. (1986). Table 2 and Fig. 4 shows that the mafic and felsic components are comparable in each sample, making it highly unlikely that the felsic grains are post-depositional (i.e., detrital) inclusions. Instead, this bimodal character appears to be a distinctive feature of the deposit. Sample means of the felsic and mafic phases show substantial overlap at one standard deviation for most element oxides, with some, but not all exceptions removed by normalization to 100% (Table 2). One-way MANOVA and *post hoc* Hotelling's T^2 tests provide a probabilistic assessment of the likelihood that the mafic and felsic glass populations from each of the three samples are correlative.

For the mafic shards, sample means overlap at one standard deviation for all element oxides of samples GS08-01, CAT08-07, and CAT06-41T except for Al_2O_3 (see Table 2 and Fig. 4). This emphasizes the strong similarities amongst the samples but suggests subtle chemical compositional differences. More formal testing using one-way MANOVA indicates that it is highly unlikely that the three mafic samples are drawn from the same population or eruption ($p < 0.0001$ for Wilk's lambda (0.18) and Pillai trace (1.10)). Pairwise comparisons using *post hoc* Hotellings T^2 tests however (Table 3), indicate that although CAT06-41T is significantly different from GS08-01 ($p < 0.0003$) and from CAT08-07 ($p = 0.0096$), neither of the latter two samples can be shown to be significantly different from one another ($p = 0.67$). These data suggest that GS08-01 and CAT08-07 are correlative, providing an isochronous link between sites KD3 and n.312. The results also suggest that CAT06-41T is similar to, yet compositionally distinct from the other samples. However, it is worth noting that all prior analyses of the bed sampled as CAT06-41T have resulted in highly variable wt. % abundances of Al_2O_3 (cf. unit R6 in Slimak et al., 2008; Tryon et al., 2009), and some of the differences may be more apparent than real, given the similarity amongst all of the other element oxides. Thus, CAT06-41T is a tentative correlate of GS08-01 and CAT08-07, following the terminology and arguments of Brown et al. (2006). All of these comparisons used raw data in their comparisons, although the same patterns held when data normalized to 100% are used.

The element oxide wt. % abundances of the felsic glass shards from samples GS08-01, CAT08-07, and CAT06-41T show substantial

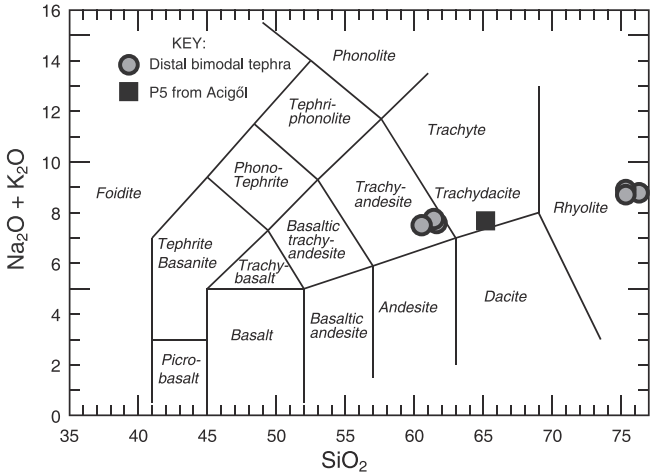

Fig. 3. Total-alkali silica diagram of Le Bas et al. (1986) showing the compositional classification of the mafic (trachyandesite) and felsic (rhyolite) phases of sample averages for GS08-01, CAT08-07, and CAT06-41T, based on electron probe microanalyses normalized to 100%. Sample P5, a "trachydacite" from Acigöl analyzed by whole-rock XRF and reported in Druitt et al. (1995), is shown for comparison.

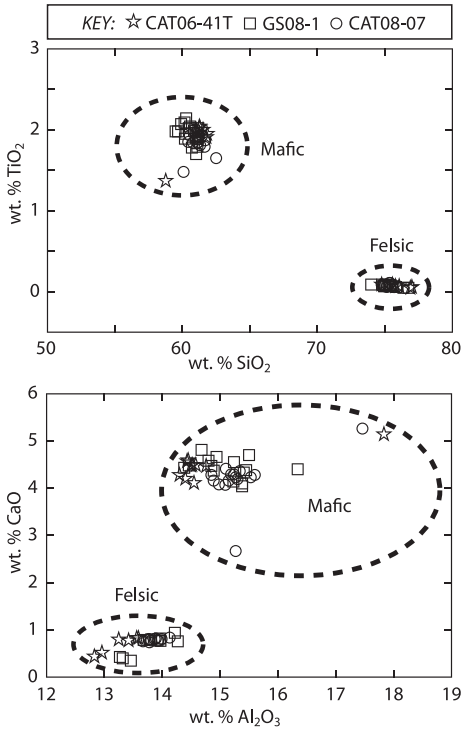

Fig. 4. Bivariate plots of weight percent (wt. %) abundances for selected elemental oxides for samples GS08-01, CAT08-07, CAT06-41T, using data normalized to 100%. Dashed lines are arbitrary.

Table 3
Pairwise Hotelling's T^2 results for mafic glasses that test for sample differences on the basis of geochemical composition. Shown are Bonferroni corrected values for multiple comparisons using non-normalized data.

	GS08-01	CAT08-07	CAT06-41T
GS08			
CAT08	0.68		
CAT06	0	0.01	

overlap among sample means. This similarity is supported by the results of one-way MANOVA tests, which fail to find strong support for the hypothesis that these glass shards derive from more than one population, using multiple statistical measures of strength with either raw (Wilk's lambda = 0.06, $p = 0.06$, Pillai trace = 1.34, $p = 0.12$) or transformed data (Wilk's lambda = 0.09, $p = 0.12$, Pillai trace = 1.27, $p = 0.20$). The felsic glass shards are correlated in all three samples. The combined similarities among the mafic and felsic glass compositions strongly suggest that the three deposits all derive from the same eruptive event.

3.4. Discussion

The bimodal nature of these mafic tephra samples has important implications for their source. Unit R6 (sample CAT06-41T) was previously hypothesized to derive from one of the many relatively small monogenetic cones in the region (Mouralis et al., 2002; Mouralis, 2003; Slimak et al., 2004, 2008; Tryon et al., 2009). The bimodal glass shards instead suggest derivation from a source with a more complex and varied compositional history. An alternative hypothesis is that these deposits derive from Acigöl volcano, ~30 km north of the sample localities (Fig. 1), supported by three lines of evidence.

First, numerous geochemical analyses by multiple laboratories strongly indicate that the five underlying tephra fallout deposits at KD3, (R1-R5) are *all* from the syn-caldera eruptions on Acigöl, known to have produced widespread eruptions of rhyolite pyroclastic deposits (Druitt et al., 1995; Mouralis et al., 2002; Mouralis, 2003; Slimak et al., 2008; Tryon et al., 2009). It is therefore plausible that overlying deposits derive from the same source.

Second, and more convincing, the felsic shards from samples GS08-01, CAT08-07, and CAT06-41T are compositionally similar to the underlying R1-R5 rhyolite glasses. Element oxide sample means of the felsic glasses (Table 2) overlap with previously published values for underlying samples R1-R5 attributed to Acigöl (Tryon et al., 2009). Discriminant analysis of these samples using the methods and reference set from Tryon et al. (2009) attribute the rhyolitic phase of *all three* of these samples to the syn-caldera eruptions at Acigöl with a posterior probability of 100% and Mahalanobis distances (D^2) of 6.89, 4.49, and 2.76, respectively. Compositional analyses of the felsic phase of these tephra therefore strongly suggest a genetic link with Acigöl, with the bimodal glass populations the result of a heterogeneous magma chamber or sampling of compositionally different deposits during magma ascent with eruption.

Third, in their study of Acigöl, both Mouralis (2003) and Druitt et al. (1995) note the presence of multiple deposits of mafic tephra stratigraphically intermediate between deposits of the rhyolitic syn- and post-caldera eruptive phases. Druitt et al. (1995: 665) termed the most widespread of these mafic deposits P5, and analyzed a sample of P5 and other deposits using whole-rock XRF analyses. Although data collected by bulk XRF techniques and EPMA may not be directly comparable, Druitt and colleagues' analyses of rhyolite pumice fragments from the syn-caldera deposits match fairly well with the microprobe analyses of rhyolite glass shards from Acigöl (see Tryon et al., 2009), suggesting that the two data sets should be broadly comparable. Tephra P5 is a trachydacite according to a whole-rock XRF analysis reported by Druitt et al. (1995), compositionally distinct from the KD3-n.312 trachyandesitic tephra (Fig. 3).

However, Druitt et al. (1995; their Table 5) note that their P5 analysis was of a single *banded pumice* [authors' emphasis]. The 2010 field observations of P5 confirm that the deposit consists of variably mafic and felsic coarse pumiceous lapilli (≤5 cm), some showing marked felsic-to-mafic compositional variation within a single clast. If the whole-rock XRF analysis of Druitt et al. (1995) did average mafic and felsic glass phases (as well as phenocrysts) within a single clast, then the resulting dacite attribution is inaccurate. Inspection of Table 2 and Fig. 3 suggests that averaging the mafic and felsic phases of the distal tephra (samples CAT06-41T, CAT08-07, and GS08-01) could produce a comparable "trachydacite" composition such as that reported by Druitt et al. (1995). Currently, testing the hypothesis of an Acigöl source for the KD3 and site n.312 tephra deposits is ongoing, through electron probe microanalyses of each of the two glass phases from multiple P5 clasts. We note that an Acigöl source is consistent with the evolution of an alkaline andesitic magma into a rhyolitic magma (Fig. 3) after fractionation of the feldspar and Fe–Ti oxide phenocrysts observed in samples GS08-01, CAT08-07, and CAT06-41T.

As stressed above, all correlations are hypotheses subject to retesting as additional data are acquired. Therefore, it is worth pointing out that including data from the analyses of the P5 proximal deposits (or whatever the source may be) into the MANOVA-based comparisons has the potential to revise the conclusions presented here. If, for example the, P5 deposit is the source of the distal tephra and it is highly variable in wt. % abundance Al_2O_3, subsequent multivariate comparisons may demonstrate that GS08-01, CAT08-07, as well as CAT06-41T all sample comparable ranges of variability among the element oxide abundance data set used here, thus further strengthening the argument for correlation. The strength of the correlation can vary with the size, and thus scale, of the comparative data set used.

4. Conclusions

Issues of scale are important in tephrostratigraphic analyses. Scalar issues range from the type of volcanic deposit studied and sampled, ranging from a volcano, to a decimeter-thick bed of tephra fallout, to individual glass shards reworked by various processes. Geochemical compositional data are also collected at scales that range from grain-discrete to bulk techniques that collect elemental abundances ranging from weight percent to parts per million. In determining which of a multitude of techniques to use to establish a correlation on the basis of these geochemical data, the scale of the question and the resolution of the data determine which method or methods are best suited to assess the probability of correlation. Drawing on examples from Paleolithic archaeological sites in Turkey shows the necessity of using different approaches to address different scales of questions from source assignment to correlating the products of a single eruption of mafic tephra, and these fine-grained approaches resulted in more robust hypotheses of source volcanoes to be tested through further analyses. Ultimately, the ability to construct sequences of correlated tephra deposits requires analytical flexibility and an increased awareness of the importance of scale.

Acknowledgments

The work reported in this paper was funded by grants from the Leakey Foundation, the Wenner-Gren Foundation, and New York University, and is the outcome of numerous discussions with and encouragement from David Lowe, Christopher Campisano, Kieran McNulty, Anthony Philpotts, Jeremy Delaney, Matthew Tocheri,

Rhonda Kauffman, and everyone at INQUA's Active Tephra in Kyushu conference. Many of the ideas here, more fully developed in Kyushu, owe their original genesis to Tryon's invitation by David Killick to speak at the National Science Foundation IGERT-funded program in Archaeological Science at the University of Arizona and the discussion that ensued. Nicholas Pearce, Lindsay McHenry, and an anonymous reviewer provided excellent comments that substantially improved the quality of the manuscript. This is a contribution towards meeting objective three of the INTREPID project of INQUA's International focus group on tephrochronology and volcanism.

Appendix 1

All microprobe analyses used in this paper, listing wt. % abundance for each element oxide, divided into mafic and felsic phases. Also reported are analyses of reference materials analyzed as unknowns to facilitate inter-laboratory comparisons. FeO_T = total Fe expressed as FeO, * Yellowstone rhyolite glass VG-568 (USNM 7285), ** Kakanui hornblende (USNM 143065); ***wet chemical analyses of these reference materials from Jarosewich et al. (1980), with FeO and Fe_2O_3 recalculated as FeO_T.

Sample	SiO_2	TiO_2	Al_2O_3	FeO_T	MnO	MgO	CaO	Na_2O	K_2O	Total
Mafic glass										
GS08-1	56.49	2.01	13.76	7.55	0.25	2.01	4.50	4.48	2.65	93.71
GS08-1	56.51	1.96	13.99	7.76	0.15	1.90	4.10	4.52	3.02	93.93
GS08-1	56.72	1.96	13.69	8.76	0.15	1.77	4.25	4.42	2.96	94.67
GS08-1	57.39	1.91	14.71	7.89	0.09	1.93	4.46	3.77	2.76	94.90
GS08-1	57.69	1.87	14.61	8.22	0.20	1.96	4.36	3.93	2.98	95.81
GS08-1	57.76	1.89	14.62	7.84	0.14	1.67	4.11	3.67	3.20	94.90
GS08-1	57.95	1.82	14.88	7.78	0.12	1.76	4.22	4.46	3.30	96.27
GS08-1	58.03	1.94	14.44	9.15	0.11	2.00	4.47	4.36	3.03	97.52
GS08-1	58.47	1.94	14.64	9.25	0.15	2.10	4.56	4.14	2.72	97.97
GS08-1	58.76	1.98	13.95	8.70	0.26	1.93	4.30	3.77	3.38	97.02
GS08-1	59.37	1.96	14.41	7.29	0.16	1.90	4.34	4.56	3.05	97.04
GS08-1	59.44	1.66	15.91	7.35	0.10	1.73	4.29	4.37	2.57	97.41
GS08-1	60.27	1.76	15.27	8.56	0.20	1.82	4.07	4.29	3.03	99.27
GS08-1	61.28	1.79	15.28	8.39	0.14	1.97	4.15	4.27	3.03	100.28
CAT08-07	57.84	1.71	14.14	7.38	0.13	2.31	3.85	4.19	2.79	94.34
CAT08-07	57.92	1.78	14.70	7.97	0.11	1.73	4.18	4.69	2.76	95.84
CAT08-07	58.63	1.71	14.52	8.16	0.12	1.22	2.54	4.37	3.85	95.11
CAT08-07	58.72	1.91	14.55	7.91	0.19	1.76	4.00	4.12	2.93	96.10
CAT08-07	58.77	1.87	14.66	7.70	0.12	1.92	4.28	4.56	3.18	97.05
CAT08-07	59.11	1.45	17.18	6.49	0.15	1.74	5.18	4.59	2.47	98.37
CAT08-07	59.22	1.78	14.62	7.40	0.21	2.01	3.94	4.70	2.98	96.86
CAT08-07	59.27	1.80	15.14	8.02	0.18	1.73	4.13	4.03	3.24	97.52
CAT08-07	59.51	1.95	14.53	8.54	0.10	1.81	4.18	4.22	3.02	97.85
CAT08-07	60.13	1.85	14.64	7.74	0.26	2.43	4.09	4.17	3.04	98.34
CAT08-07	60.15	1.83	14.81	7.19	0.21	1.77	4.18	4.19	3.17	97.52
CAT08-07	60.25	1.81	15.06	7.52	0.06	1.76	4.17	4.90	3.05	98.58
CAT08-07	60.43	1.88	15.05	7.65	0.29	1.95	4.23	4.51	2.76	98.74
CAT08-07	61.72	1.63	15.41	6.38	0.14	1.64	4.22	4.67	2.93	98.76
CAT06-41T_2010	57.41	1.76	13.65	7.95	0.21	1.88	3.86	4.12	2.98	93.83
CAT06-41T_2010	58.00	1.93	13.81	7.59	0.15	2.00	4.25	4.30	2.65	94.67
CAT06-41T_2010	58.16	1.81	14.04	7.57	0.16	1.84	4.26	4.87	2.43	95.13
CAT06-41T_2010	59.48	1.97	14.02	7.88	0.08	2.02	4.46	4.23	2.91	97.05
CAT06-41T_2010	60.04	1.90	14.08	7.38	0.18	1.76	4.35	4.83	2.57	97.10
CAT06-41T_2010	60.36	1.97	14.15	7.71	0.06	1.87	4.48	4.86	2.63	98.09
CAT06-41T_2010	60.53	1.97	14.40	8.64	0.18	1.93	4.45	4.12	2.95	99.20
CAT06-41T_2010	60.58	1.98	14.20	8.67	−0.01	1.71	4.25	5.14	2.74	99.28
CAT06-41T_2010	60.60	1.88	14.12	7.75	0.11	2.04	4.12	4.03	3.44	98.09
Felsic glass										
GS08-1	70.04	0.08	13.32	0.96	0.07	0.05	0.71	3.55	4.56	93.34
GS08-1	70.42	0.07	13.05	1.02	0.06	0.07	0.77	3.74	4.27	93.46
GS08-1	71.50	0.05	12.61	0.74	0.07	0.02	0.33	3.85	4.48	93.64
GS08-1	72.00	0.07	13.27	1.31	0.02	0.04	0.77	3.83	4.77	96.08
GS08-1	72.04	0.08	13.34	1.09	0.06	0.05	0.74	3.75	4.37	95.52
GS08-1	72.06	0.08	13.18	1.31	0.15	0.07	0.76	4.29	4.45	96.35
GS08-1	72.08	0.04	12.47	0.61	0.04	0.02	0.40	3.76	4.53	93.95
GS08-1	72.24	0.09	13.89	1.51	0.16	0.06	0.92	4.11	4.66	97.65
CAT08-07	70.30	0.07	12.91	1.20	0.05	0.06	0.76	3.86	4.57	93.78
CAT08-07	70.68	0.06	13.04	0.87	0.09	0.05	0.72	3.71	4.36	93.56
CAT08-07	71.21	0.09	13.09	1.22	0.22	0.04	0.74	3.87	4.27	94.73
CAT08-07	71.41	0.07	12.96	0.76	0.01	0.05	0.69	3.87	4.26	94.07
CAT08-07	71.44	0.10	12.96	1.16	0.04	0.07	0.72	3.43	4.90	94.80
CAT06-41T_2010	71.85	0.08	12.60	1.53	0.06	0.04	0.76	3.90	4.29	95.11
CAT06-41T_2010	72.52	0.07	12.98	0.79	0.06	0.05	0.79	4.14	4.31	95.71
CAT06-41T_2010	72.58	0.07	12.81	0.87	0.03	0.07	0.75	3.78	4.50	95.43
CAT06-41T_2010	73.09	0.06	12.31	0.64	0.06	0.02	0.49	3.68	4.60	94.94
CAT06-41T_2010	73.34	0.04	12.24	0.66	0.10	0.01	0.42	4.00	4.59	95.40
Reference materials analyzed as unknowns										
Glass VG-568*	75.68	0.09	12.52	1.11	0.04	0.01	0.42	3.80	5.28	98.94
Glass VG-568*	75.89	0.08	12.51	1.33	0.00	0.02	0.44	3.60	4.87	98.72
Glass VG-568*	75.63	0.09	12.43	1.24	−0.06	0.02	0.41	3.80	5.00	98.56
Glass VG-568*	75.56	0.08	12.34	1.05	0.14	0.01	0.44	3.86	4.95	98.41

(continued on next page)

(*continued*)

Sample	SiO_2	TiO_2	Al_2O_3	FeO_T	MnO	MgO	CaO	Na_2O	K_2O	Total
Glass VG-568*	77.13	0.07	12.58	1.11	0.07	0.01	0.46	3.87	5.45	100.75
Glass VG-568*	79.52	0.08	12.87	1.71	0.04	0.01	0.45	3.61	4.86	103.15
Glass VG-568*	78.03	0.06	12.62	0.98	0.08	0.02	0.43	3.85	5.05	101.11
Glass VG-568*	77.39	0.10	12.50	1.34	0.09	0.00	0.47	3.83	5.06	100.78
Glass VG-568*	74.91	0.05	12.44	1.02	0.01	0.02	0.41	3.57	5.13	97.55
Glass VG-568***	76.71	0.12	12.06	1.23	0.03	<0.1	0.50	3.75	4.89	99.30
Kakanui hornblende**	41.02	4.80	14.85	12.01	0.03	12.77	10.35	2.60	2.16	100.58
Kakanui hornblende**	41.36	4.77	15.16	12.20	0.14	12.62	10.60	2.60	2.11	101.56
Kakanui hornblende**	41.78	4.83	14.88	11.88	0.12	12.90	10.36	2.81	2.12	101.70
Kakanui hornblende**	40.59	4.78	15.06	11.67	0.11	12.71	10.35	2.72	2.05	100.04
Kakanui hornblende**	39.91	4.82	14.63	10.89	0.11	12.63	10.52	2.49	2.09	98.10
Kakanui hornblende***	40.37	4.72	14.90	10.92	0.09	12.80	10.30	2.60	2.05	98.75

References

Armstrong, J.T., 1988. Quantitative analysis of silicate and oxide materials: Comparison of Monte Carlo, ZAF, and $\phi(\rho z)$. In: Newbury, D.E. (Ed.), Microbeam Analysis-1988. San Francisco Press, Inc., San Francisco, pp. 239–246.

Balkan-Atlı, N., Kuhn, S., Astruc, L., Çakan, G., Dinçer, B., Kayacan, N., 2008. Göllü Dağ 2007 survey. Anatolia Antiqua 16, 293–312.

Balkan-Atlı, N., Kuhn, S.L., Astruc, L., Kayakan, N., Dinçer, B., Çakan, G., 2009. Göllü Dağ 2008 survey. Anatolia Antiqua 17, 301–315.

Baxter, M.J., 1994. Exploratory Multivariate Analysis in Archaeology. Edinburgh University Press, Edinburgh.

Borchardt, G.A., Aruscavage, P.J., Millard, H.T.J., 1972. Correlation of the Bishop Ash, a Pleistocene marker bed, using instrumental neutron activation analysis. Journal of Sedimentary Petrology 42, 301–306.

Bourne, A.J., Lowe, J.J., Trincardi, F., Asioli, A., Blockley, S.P.E., Wulf, S., Matthews, I.P., Piva, A., Vigliotti, L., 2010. Distal tephra record for the last ca 105,000 years from the core PRAD 1-2 in the central Adriatic Sea: implications for marine tephrostratigraphy. Quaternary Science Reviews 29, 3079–3094.

Brown, F.H., Haileab, B., McDougall, I., 2006. Sequence of tuffs between the KBS Tuff and the Chari Tuff in the Turkana Basin, Kenya and Ethiopia. Journal of the Geological Society 163, 185–204. London.

Brown, F.H., Sarna-Wojcicki, A.M., Meyer, C.E., Haileab, B., 1992. Correlation of Pliocene and Pleistocene tephra layers between the Turkana Basin of East Africa and the Gulf of Aden. Quaternary International 13/14, 55–67.

Campisano, C.J., Feibel, C.S., 2008. Tephrostratigraphy of the Hadar and Busidima Formations at Hadar, Afar Depression, Ethiopia. In: Quade, J., Wynn, J.G. (Eds.), The Geology of Early Humans in the Horn of Africa. Geological Society of America Special Paper 446. Boulder, CO, pp. 135–162.

Cerling, T.E., Brown, F.H., Bowman, J.R., 1985. Low-temperature alteration of volcanic glass: Hydration, Na, K, ^{18}O and Ar mobility. Chemical Geology 52, 281–293.

Chauhan, P.R., 2010. Comment on 'Lower and Early Middle Pleistocene Acheulian in the Indian sub-continent' Gaillard et al. (2009) (Quaternary International). Quaternary International 223-224, 248–259.

Deniel, C., Aydar, E., Gourgaud, A., 1998. The Hasan Dagi stratovolcano (Central Anatolia, Turkey): evolution from calc-alkaline to alkaline magmatism in a collision zone. Journal of Volcanology and Geothermal Research 87, 275–302.

Denton, J.S., Pearce, N.J.G., 2008. Comment on "A synchronized dating of three Greenland ice cores throughout the Holocene" by B.M. Vinther et al.: no Minoan tephra in the 1642 B.C. layer of the GRIP core. Journal of Geophysical Research 113, D04303.

Donovan, J.J., Kremser, D., Fournelle, J., 2009. Probe for EPMA: Acquisition, Automation and Analysis. Enterprise Edition. Probe Software, Inc., Eugene.

Druitt, T.H., Brenchley, P.J., Gökten, Y.E., Francaviglia, V., 1995. Late Quaternary rhyolitic eruptions from the Acigöl complex, central Turkey. Journal of the Geological Society 152, 655–667. London.

Fedele, F.G., Giaccio, B., Hajdas, I., 2008. Timescales and cultural processes at 40,000 BP in the light of the Campanian Ignimbrite eruption, Western Eurasia. Journal of Human Evolution 55, 834–857.

Feldesman, M.R., 1997. Bridging the chasm: Demystifying some statistical methods used in biological anthropology. In: Boaz, N., Wolfe, L. (Eds.), Biological Anthropology: The State of the Science, second ed. IIHER and Oregon State University, Corvallis, OR, pp. 73–100.

Fisher, R.A., 1936. The use of multiple measurements in taxonomic problems. Annals of Eugenics 7, 179–188.

Froggatt, P.C., 1992. Standardization of the chemical analysis of tephra deposits. Report of the ICCT Working Group. Quaternary International 13/14, 93–96.

Hammer, Ø, Harper, D.A.T., Ryan, P.D., 2001. PAST: Paleontological Statistics software package for education and data analysis. Palaeontologica Electronica 4, 9. art 4.

Hunt, J.B., Hill, P.G., 1993. Tephra geochemistry: a discussion of some persistent analytical problems. The Holocene 3, 272–278.

Hunt, J.B., Hill, P.G., 1996. An inter-laboratory comparison of the electron probe microanalysis of glass geochemistry. Quaternary International 34-36, 229–241.

Hunt, J.B., Hill, P.G., 2001. Tephrological implications of beam size-sample size effects in electron microprobe analysis of glass shards. Journal of Quaternary Science 16, 105–117.

Innocenti, F., Mazzuoli, R., Pasquaré, G., Villari, L., 1982. Anatolia and north-western Iran. In: Thorpe, R.S. (Ed.), Andesites. John Wiley and Sons, New York, pp. 327–349.

Jarosewich, E., Nelson, J.A., Norbers, J.A., 1980. Reference samples for electron microprobe analysis. Geostandards Newsletter 4, 43–47.

Jarosewich, E., Parkes, A.S., Wiggins, L.B., 1979. Microprobe analyses of four natural glasses and one mineral: an interlaboratory study of precision and accuracy. Smithsonian Contributions to the Earth Sciences 22, 53–67.

Jensen, B.J.L., Froese, D.G., Preece, S.J., Westgate, J.A., Stachel, T., 2008. An extensive middle to late Pleistocene tephrochronologic record from east-central Alaska. Quaternary Scicence Reviews 27, 411–427.

Kappelman, J., Alçiçek, M., Kazanci, N., Schultz, M., Özkul, M., Sen, Ş, 2007. Brief communication: first *Homo erectus* from Turkey and implications for migrations into temperate Eurasia. American Journal of Physical Anthropology 135, 110–116.

Keenan, D.J., 2003. Volcanic ash retrieved from the GRIP ice core is not from Thera. Geochemistry, Geophysics. Geosystems 4, 1–8.

Kuehn, S.C., Foit Jr., F.F., 2006. Correlation of widespread Holocene and Pleistocene tephra layers from Newberry Volcano, Oregon, USA, using glass compositions and numerical analysis. Quaternary International 148, 113–137.

Kuehn, S.C., Froese, D., Shane, P.A. The INTAV intercomparison of electron-beam microanalysis of glass by tephrochronology laboratories, results and recommendations. Quaternary International, this issue.

Kuhn, S.L., 2002. Paleolithic archaeology in Turkey. Evolutionary Anthropology 11, 198–210.

Kuhn, S.L., 2009. Was Anatolia a bridge or a barrier to early hominin dispersals? Quaternary International 223/224, 434–435.

Kuhn, S.L., Stiner, M.C., Gülec, E., Özer, I., Yılmaz, H., Baykara, I., Açıkkol, A., Goldberg, P., Martínez Molina, K., Ünay, E., Suata-Alpaslan, F., 2009. The early upper Paleolithic occupations of Üçağızlı Cave (Hatay, Turkey). Journal of Human Evolution 56, 87–113.

Le Bas, M.J., Le Maitre, R.W., Streckeisen, A., Zanettin, B., 1986. A chemical classification of volcanic rocks based on the total alkali-silica diagram. Journal of Petrology 27, 745–750.

Lowe, D.J., 2011. Tephrochronology and its application: a review. Quaternary Geochronology 6, 107–153.

McHenry, L.J., Mollel, G.F., Swisher III, C.C., 2008. Compositional and textural correlations between Olduvai Gorge bed I tephra and volcanic sources in the Ngorongoro volcanic Highlands, Tanzania. Quaternary International 178, 306–319.

McHenry, L.J., Luque, L., Gómez, J.Á, Diez-Martín, F., 2011. Promise and pitfalls for characterizing and correlating the zeolitically altered tephra of the Pleistocene Peninj Group, Tanzania. Quaternary Research 75, 708–720.

Mouralis, D., 2003. Les complexes volcaniques quaternarires de Cappadoce (Göllüdağ et Acigöl) – Turquie: Évolutions morphodynamiques et implications environnementales. Paris, Université Paris 12. Thèse de Doctorat.

Mouralis, D., Pastre, J.-F., Kuzucuoğlu, C., Türkecan, A., Atici, Y., Slimak, L., Guillou, H., Kunesch, S., 2002. Les complexes volcaniques rhyolitiques quaternaires d'Anatolie centrale (Göllü Dag et Acigöl, Turquie): Genèse, instabilité, contraintes environnementales. Quaternaire 13, 219–228.

Neff, N.A., Marcus, L.F., 1980. A Survey of Multivariate Methods for Systematics. Privately published, New York.

Otte, M., Yalçinkaya, I., Kozlowski, J., Bar-Yosef, O., López Bayón, I., Taskiran, H., 1998. Long-term technical evolution and human remains in the Anatolian Palaeolithic. Journal of Human Evolution 34, 413–431.

Pearce, N.J.G., Denton, J.S., Perkins, W.T., Westgate, J.A., Alloway, B.V., 2007. Correlation and characterization of individual glass shards from tephra deposits using trace element laser ablation ICP-MS analyses: current status and future potential. Journal of Quaternary Science 22, 721–736.

Pearce, N.J.G., Bendall, C.A., Westgate, J.A., 2008. Comment on "Some numerical considerations in the geochemical analysis of distal microtephra" by A.M. Pollard, S.P.E. Blockley and C.S. Lane. Applied Geochemistry 23, 1353–1364.

Perkins, M.E., Nash, W.P., Brown, F.H., Fleck, R.J., 1995. Fallout tuffs of Trapper Creek, Idaho: a record of Miocene explosive volcanism in the Snake River Plain volcanic province. Geological Society of America Bulletin 107, 1484–1506.

Pollard, A.M., Blockley, S.P.E., Lane, C.S., 2006. Some numerical considerations in the geochemical analysis of distal microtephra. Applied Geochemistry 21, 1692–1714.

Preece, S.J., Pearce, N.J.G., Westgate, J.A., Froese, D.G., Jensen, B.J.L., Perkins, W.T., in press. Old Crow tephra across eastern Beringia: a single cataclysmic eruption at the close of Marine Isotope Stage 6. Quaternary Science Reviews. Doi:10.1016/j.quascirev.2010.04.020

Riehle, J.R., Ager, T.A., Reger, R.D., Pinney, D.S., Kaufman, D.S., 2008. Stratigraphic and compositional complexities of the late Quaternary Lethe tephra in South-central Alaska. Quaternary International 178, 210–228.

Sarna-Wojcicki, A.M., Bowman, H.R., Meyer, C.E., Russell, P.C., Woodward, M.J., McCoy, G., Rowe Jr., J.J., Baedecker, P.A., Asaro, F., Michael, H., 1984. Chemical Analyses, Correlations, and Ages of Upper Pliocene and Pleistocene Ash Layers of East-Central and Southern California. United States Geological Survey Professional Paper 1293, Washington, DC.

Schmid, R., 1981. Descriptive nomenclature of classification of pyroclastic deposits and fragments: Recommendations of the IUGS Subcommission on the Systematics of Igneous Rocks. Geology 9, 41–43.

Shane, P.A.R., Nairn, I.A., Martin, S.B., Smith, V.C., 2008. Compositional heterogeneity in tephra deposits resulting from the eruption of multiple magma bodies: implications for tephrochronology. Quaternary International 178, 44–53.

Slimak, L., Roche, H., Mouralis, D., Buitenhuis, H., Balkan-Atli, N., Binder, D., Kuzucuoğlu, C., Grenet, M., 2004. Kaletepe Deresi 3 (turquie), aspects archéologiques, chronologiques et paléontologiques d'une sequence pléistocène en Anatolie centrale. Comptes Rendus Palevol 3, 411–420.

Slimak, L., Kuhn, S.L., Roche, H., Mouralis, D., Buitenhuis, H., Balkan-Atli, N., Binder, D., Kuzucuoğlu, C., Guillou, H., 2008. Kaletepe Deresi 3 (Turkey): archaeological evidence for early human settlement in central Anatolia. Journal of Human Evolution 54, 99–111.

Smith, V.C., Pearce, N.J.G., Matthews, N.E., Westgate, J.A., Petraglia, M.D., Haslam, M., Lane, C.S., Korisettar, R., Pal, J.N., 2011. Geochemical fingerprinting of the widespread Toba tephra using biotite compositions. Quaternary International 246, 97–104.

Stern, N., 1993. The structure of the Lower Pleistocene archaeological record. Current Anthropology 34, 201–225.

Stokes, S., Lowe, D.J., 1988. Discriminant function analysis of late Quaternary tephras from five volcanoes in New Zealand using glass shard major element chemistry. Quaternary Research 30, 270–283.

Stokes, S., Lowe, D.J., Froggatt, P.C., 1992. Discriminant function analysis and correlation of late Quaternary rhyolitic tephra deposits from Taupo and Okatina volcanoes, New Zealand, using glass shard major element composition. Quaternary International 13/14, 103–117.

Tiercelin, J.-J., Schuster, M., Roche, H., Brugal, J.-P., Thuo, P., Prat, S., Harmand, S., Davitan, G., Barrat, J.-A., Bohn, M., 2010. New considerations on the stratigraphy and environmental context of the oldest (2.34 Ma) Lokalalei archaeological site complex of the Nachukui Formation, West Turkana, northern Kenya Rift. Journal of African Earth Sciences 58, 157–184.

Tryon, C.A., Faith, J.T., Peppe, D.J., Fox, D.L., Holt, K., Dunsworth, H., Harcourt-Smith, W., 2010. The Pleistocene archaeology and environments of the Wasiriya beds, Rusinga Island, Kenya. Journal of Human Evolution 59, 657–671.

Tryon, C.A., Logan, M.A.V., Mouralis, D., Kuhn, S.L., Slimak, L., Balkan-Atlı, N., 2009. Building a tephrostratigraphic framework for the Paleolithic of central Anatolia, Turkey. Journal of Archaeological Science 36, 637–652.

Tryon, C.A., McBrearty, S., 2002. Tephrostratigraphy and the Acheulian to Middle Stone Age transition in the Kapthurin Formation, Baringo, Kenya. Journal of Human Evolution 42, 211–235.

Tryon, C.A., McBrearty, S., 2006. Tephrostratigraphy of the Bedded Tuff Member (Kapthurin Formation, Kenya) and the nature of archaeological change in the later middle Pleistocene. Quaternary Research 65, 492–507.

Tryon, C.A., Roach, N.T., Logan, M.A.V., 2008. The Middle Stone Age of the northern Kenyan Rift: age and context of new archaeological sites from the Kapedo tuffs. Journal of Human Evolution 55, 652–664.

Turney, C.S.M., Blockley, S.P.E., Lowe, J.J., Wulf, S., Branch, N.P., Mastrolorenzo, G., Swindle, G., Nathan, R., Pollard, A.M., 2008. Geochemical characterization of quaternary tephras from the Campanian province, Italy. Quaternary International 178, 288–305.

Weigand, P.C., Harbottle, G., Sayre, E.V., 1977. Turquoise sources and source analysis: Mesoamerican and Southwestern USA. In: Earle, T.K., Ericson, J.E. (Eds.), Exchange Systems in Prehistory. Academic Press, New York, pp. 15–34.

Westgate, J.A., Shane, P.A.R., Pearce, N.J.G., Perkins, W.T., Korisettar, R., Chesner, C.A., Williams, M.A.J., Acharyya, S.K., 1998. All Toba tephra occurrences across Peninsular India belong to the 75,000 yr B.P. eruption. Quaternary Research 50, 107–112.

Williams, M.A.J., Ambrose, S.H., van der Kaars, S., Ruehlmann, C., Chattopadhyaya, U., Pal, J., Chauhan, P.R., 2009. Environmental impact of the 73 ka Toba super-eruption in South Asia. Palaeogeography, Palaeoclimatology, Palaeoecology 284, 295–314.